INFLUENCE OF STRESS RANGE ON PLAIN CONCRETE PAVEMENT FATIGUE DESIGN

Lorenzo Domenichini and Aurelio Marchionna, Research Engineers,
Università di Roma

A concrete pavement fatigue design procedure accounting for the strees range induced by the applied loads is proposed. As a matter of fact the stress range, whose value is variable in time as temperature and traffic stresses in the pavement vary, affects the concrete fatigue strength and laboratory fatigue laws accounting for such a parameter have been defined.
The Tepfers's fatigue law has been checked and corrected according, to the experimental results of the AASHO Road Test. The structural analysis of several concrete AASHO sections has been performed superimposing the seasonal and dayly variations of the warping stresses with the traffic induced stresses and imposing that the cumulative damage up to failure induced by the effective number of repetitions associated to each resultant stress condition satisfies the Miner's law. A corrected design fatigue law is therefore proposed and some practical design suggestions are developped based on the analysis of the influence of the stress range.

Laboratory fatigue tests have shown that concrete fatigue strength is affected by the minimum value of the fluctuating stress applied. Most of the fatigue laws applied in pavement design result from tests performed with $\sigma_{min} \simeq 0$; on the other hand the stress conditions in a concrete pavement due to traffic loads and temperature vary between a maximum value and a minimum value which is different from zero during most of the time. As a matter of fact, when traffic stresses appear, they add themselves to the existing temperature stresses. In order to account for this condition, reference must be made to a fatigue law in which fatigue behaviour depends on the ratio: $R = \sigma_{min} / \sigma_{max}$ where σ_{min} = lower limit of repeated stress, and σ_{max} = upper limit of repeated stress.

Fatigue Behaviour of Plain Concrete Pavements

Fatigue failure induced by traffic load repetitions is one of the basic structural distresses which affect the performance of highway pavements. Based on this limiting design criterion, the Portland Cement Association has proposed a well known thickness design procedure for concrete pavements (3) based on the theoretical stress analysis by Pickett and Ray (4) of the stresses induced by traffic and on a fatigue curve obtained from the most conservative results of several fatigue studies (5).

A similar approach has been proposed by other Authors (6, 7, 8, 9), who have added to traffic stresses thermal warping stresses. The fatigue curves adopted in such design procedures are shown in Figure 1.

A factor which is not accounted for in the previously mentioned design procedures, concerns the influence experimentally observed in laboratory tests of the range between the upper and lower limits of the fluctuating stress on the concrete fatigue strength. Figure 2 shows two curves obtained from tests with loads ranging between a minimum and a maximum value whose ratio is 0.15 and 0.75 respectevely (10). From this diagram it is evident that a decrease of the stress ratio results in a decreased fatigue resistance. In concrete pavements this actually occurs: the stresses vary between a minimum value σ_{min}, corresponding to the warping stress (σ_w) whose fluctuating cycle is very slow, and a maximum value σ_{max} equal to the former added with the stresses induced by traffic loads (σ_t) whose fluctuations are rapid.

Therefore with reference to Figure 3, the following stress ratio can be defined:

$$R = \frac{\sigma_{min}}{\sigma_{max}} = \frac{\sigma_w}{\sigma_w + \sigma_t} \qquad (1)$$

Figure 1. Concrete fatigue curves.

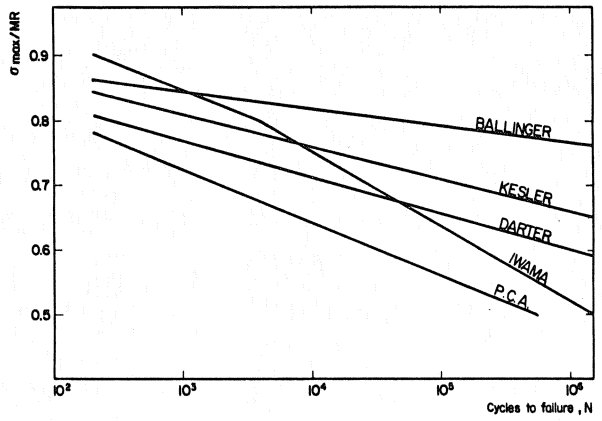

Figure 2. Influence of ratio R on concrete fatigue strength.

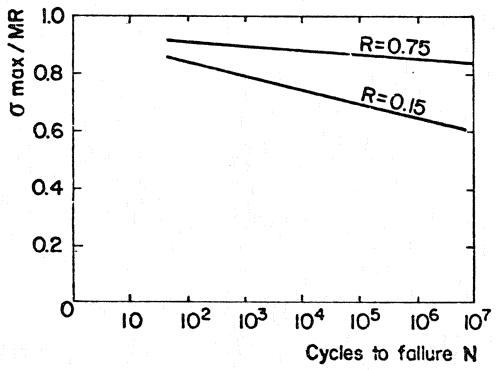

Figure 3. Schematic stress cycles in a concrete pavement.

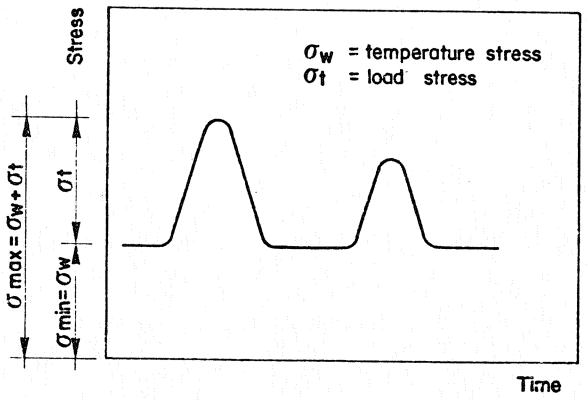

The value of R is variable in time as temperature and traffic stresses vary.

Since the critical stress condition in the slabs occurs when the warping stresses are due to positive thermal gradients, i.e. the temperature of the surface is higher than the temperature of the bottom (daytime condition), in this paper the lower limit of the repeated stress is considered always positive ($\sigma_{min} \geq 0$) as well as the ratio R.

To represent the influence on the pavement design of the ratio R as a function of the ratios σ_t/MR and σ_w/MR the diagram of Figure 4 has been developed, where MR is the Concrete Modulus of Rupture. Line (a), whose equation is:

$$\frac{\sigma_t + \sigma_w}{MR} = \frac{\sigma_{max}}{MR} = 0.5 \qquad (2)$$

divides the plane of the diagram in two areas, A and B, which respectively represent the stress conditions producing fatigue damage in concrete pavements, and the stress conditions which do not produce such damage, i.e. stress conditions below the endurance limit corresponding to a stress ratio $\sigma_{max}/MR = 0.5$. Line (b) represents all the stress conditions in the pavement due to the superimposition of the max. induced traffic load stress (e.g. $\frac{\sigma_{t,max}}{MR} = 0.35$) and the warping stresses variable between zero and $\sigma_{w,max}$, while line (c) represents all possible combinations of the max. warping stress (e.g. $\frac{\sigma_{w,max}}{MR} = 0.30$) with the stresses induced by all the traffic loads riding on the pavement. All the possible stress conditions in the slab are represented by points located in the rectangular area delimited by such lines. However only stress conditions located in the shaded area of the diagram are those which should be considered as causing fatigue damage. Any straight line departing

Figure 4. Min. and max. values of ratio R of all the possible stress conditions causing fatigue damage in a pavement.

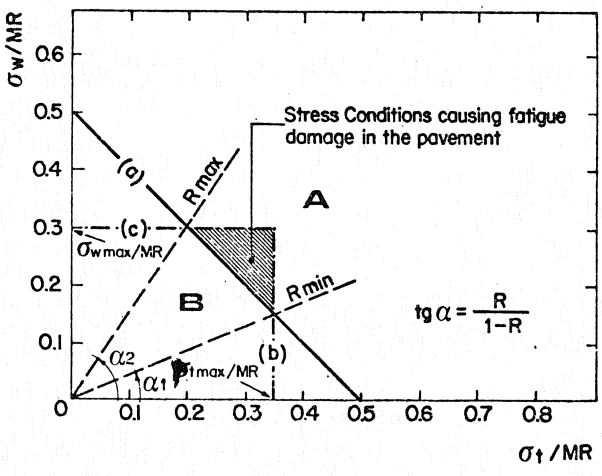

from the origin and having equation:

$$\frac{\sigma_w}{MR} = \frac{R}{1-R} \cdot \frac{\sigma_t}{MR} \qquad (3)$$

represents stress conditions characterized by constant R ratios. Those corresponding to the maximum and the minimum values of R, within which the stress conditions producing fatigue are included, are shown with dashed lines. These limiting values of R are:

$$R_{max} = \frac{\sigma_{w,max}}{0.5\ MR} \qquad (4)$$

and

$$R_{min} = 1 - \frac{\sigma_{t,max}}{0.5\ MR} \qquad (5)$$

and depend only on the safety factor relative to max traffic stress.

Thus from Figure 4 and equation 5, we can deduce that as the ratio $\sigma_{t,max}/MR$ increases, while the ratio $\sigma_{w,max}/MR$ remains constant, the value of R min decreases and consequently the area containing the stress conditions resulting in fatigue increases. More specifically, if in a pavement design we adopt a safety factor of 2 with respect to traffic loads, we obtain $\sigma_{t,max}/MR = 0.5$ and R min. = 0. This is the most unfavourable condition which exists with respect to fatigue life. To obtain a value of R min higher than zero, a safety factor higher than 2.0 must be adopted. For instance, R min = 0.2 can be obtained with a safety factor of 2.5.

Introduction of Ratio R in The Design Curves

Laboratory fatigue curves for concrete have usually been obtained from fatigue tests in which the value of σ_{min} has been maintained always very low, near to zero; anyhow R was always less or equal to 0.15. Such fatigue curves found by Ballinger (11) and Kesler (12) are shown in Figure 1. Only recently, fatigue tests have been performed by Tepfers (1, 2) on concrete specimens subjected both to compressive and to tensile stresses at different R values. The fatigue law proposed by him is:

$$\frac{\sigma_{max}}{f'_c} = 1 - \beta\,(1-R)\log_{10} N \qquad (6)$$

Figure 5. Fatigue curves for constant value of R.

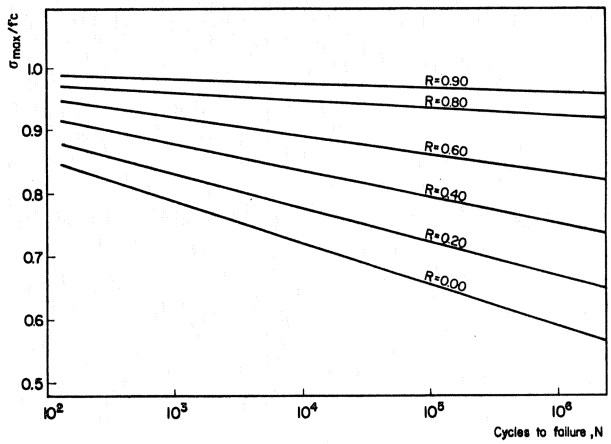

in which:

f'_c = compressive or tensile strength

β = a coefficient, whose value proposed by Tepfers is 0.0685

$R = \sigma_{min} / \sigma_{max}$

N = number of loading cycles producing failure

Equation 6 is represented by a series of straight lines on Wohler's stress - fatigue life diagram. Each line corresponds to a constant value of R (see Figure 5).

As it has been experimentally confirmed that the fatigue laws of plain concrete are essentially the same in compression, tension or flexure, equation 6 can be assumed to represent fatigue properties of plain concrete when subjected to flexural stresses as well. Therefore the use of a fatigue law of the type

Figure 6. Goodman-Smith diagram proposed by Eisenman for the fatigue design of concrete pavements.

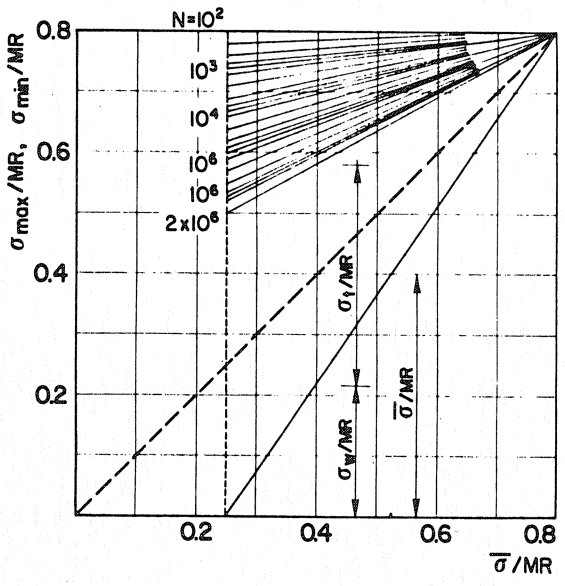

shown in equation 6 in the design procedure is proposed.

A fatigue design procedure which includes the influences of the stress range has already been proposed by Eisenmann (13) using the simplified Goodman - Smith diagram shown in Figure 6. Such a diagram has been obtained on the basis of the PCA fatigue curve increased to $2x10^6$ number of allowable repetitions at a stress ratio equal to 0.51 and assumed to provide the concrete fatigue strenght related to a stress cycle with $\sigma_{min}=0$ (R = 0).

Tepfer's law now enables us to account for the effective influence of the stress range on the fatigue properties of the concrete. However, it is not possible to directly use the fatigue law 6 in concrete pavement fatigue design, as the fatigue life of concrete determined in the laboratory is not directly comparable to the actual fatigue performance of a pavement. Among the reasons which induce to consider a difference between the actual pavement fatigue life and the one presumed on the basis of concrete laboratory fatigue tests, the following may be listed:

1. Different stress conditions and different accuracy levels in the applied loads; for instance, σ_{min} is constant in a laboratory test while σ_{min} is variable in the field.
2. Rest periods in the field, generally absent in laboratory testing;
3. Greater variability in the field of parameters affecting fatigue life (pavement thickness, Concrete Modulus of Rupture, etc.);
4. Different definition of fatigue failure: under traffic conditions fatigue failure is related to a certain extension of cracking while in a laboratory test it is related to sample collapse.
5. Approximation of Miner's law used in pavement design.

Some of the above listed reasons result in an increase in the pavement fatigue life; others in a decrease. In general, these considerations have led to the adoption of fatigue design curves more conservative than those obtained from laboratory tests (see Figure 1, Ballinger and Kesler).

Thus a correction of equation 6 is deemed necessary. This can be done by modifying the value of coefficient β . An effective means to achieve this purpose is to make reference to the experimental results of the AASHO road test (14).

The corrected value of coefficient β has been determined according to the following procedure:

1. Evaluation of load stresses in the AASHO pavement sections by means of Westergaard's edge stress equation (15);
2. Evaluation of the thermal gradients by means of Thomlinsons's heat diffusion model (16);
3. Evaluation of temperature stresses by means of Eisenmann's approach (13);
4. Determination of the values of the ratios σ_{max}/MR and R and their introduction in equation 6.;
5. Evaluation of the corrected β value imposing that the effective value of the number of repetitions to failure (Cracking index = 0.16 m/m^2 or 50 ft/1000 sq.ft.) satisfies Miner's law (17).

Stress Analysis of AASHO Pavements

Sections Selected.

To distinguish fatigue failure from other distress phenomena, the fatigue failure of a pavement may be defined as the condition in which the Cracking Index C' (total lenght of all cracks per unit pavement area (14)) has a low value such as 0.16 m/m^2 (50 ft/1000 sq.ft.). At such a cracking level, it may be presumed that no other distress phenomena have arisen, such as to modify the calculated stress conditions. During the AASHO Road Test, when the value of the C'=0.16 m/m^2 , the corresponding PSI value was not, in general, lower than 4 and the cracks were of class 1 and 2.

Table 1. Selected AASHO pavements.

Loop	Lane	Sect.	Thickness cm (in) Slab	Thickness cm (in) Subbase	Axle load kN (kips)		Unweighted Axle applications up to C'=0.16 m/m^2 (50 ft/1000 ft^2)
2	2	806	6,3 (2,5)	0	27,24 (6)	S[a]	300.712
2	2	814	8,9 (3,5)	0	27,24 (6)	S	1.017.047
4	1	643	12,7 (5,0)	7,6 (3)	81,72 (18)	S	644.169
3	2	220	12,7 (5,0)	22,9 (9)	145,28 (32)	T[b]	682.771
5	1	513	16,5 (6,5)	7,6 (3)	101,70 (22,4)	S	724.686
6	2	354	20,3 (8,0)	7,6 (3)	217,92 (48)	T	1.038.312
5	1	507	20,3 (8,0)	22,9 (9)	101,70 (22,4)	S	1.110.577
5	2	508	20,3 (8,0)	22,9 (9)	181,60 (40)	T	850.891
5	1	525	24,1 (9,5)	15,2 (6)	101,70 (22,4)	S	1.220.225

[a] S = Single Axle

[b] T = Tandem Axle

The importance of separating the fatigue phenomenon from other distress phenomena is so much greater when, as is the present case, the relationship existing between fatigue resistance and stress conditions is examined in greater detail by means of the stress range. It should however be born in mind that, during the AASHO Road Test, once the C' value = 0.16 m/m^2 has been reached, the pavements showed a residual life of approx. 25-30 per cent before attaining the limit of a PSI value of 2.5.

On the basis of this consideration, the plain concrete AASHO sections which had reached a C' value of 0.16 m/m^2 were examined. The number of allowable repetitions corresponding to C'=0.16 m/m^2, when not directly available from AASHO test results, was extrapolated from the closest available value. The Authors have limited themselves to the extrapolation of values corresponding to C' between 0.13 and 0.19 m/m^2 (40-60 ft/1000 sq.ft). This chosen criterion has reduced the total number of sections to those shown in Table 1, on which this study is based.

The pavement thickness (slab and subbase), the traffic load stresses and the number of load repetitions corresponding to a C' value equal to 0.16 m/m^2 (50 ft/1000 sq.ft) appear in the same Table.

Traffic Load Stresses

The examination of the cracks pattern in the AASHO pavements (18) has shown that the cracking of the thinner pavements (thickness 6.3-8.9 cm, 2.5"-3.5"), in general, developped itself perpendicularly to the transverse joint, originating from the joint itself. Thus the critical stress conditions were those parallel to the transverse joint. In the thicker pavements, instead, the cracks originated from the free edge and therefore the critical stresses were those parallel to the edge.

The critical traffic load stresses were therefore calculated using the edge Westergaard equation (15).

The stress values calculated using this equation were reduced by 25 percent so as to account for the presence of the dowel bars in the transverse joint

Table 2. Traffic stresses in AASHO pavements accorgind to Westergaard edge equation

Loop	Lane	Sect.	Traffic Stress σ_t (MPa)
2	2	806	3,00
2	2	814	1,80
4	1	643	2,26[a]
3	2	220	2,01
5	1	513	2,15
6	2	354	1,65
5	1	507	1,56
5	2	508	1,42
5	1	525	1,19

[a] measured value according to (18)

Figure 7. Average maximum and minimum dayly temperature per month during the AASHO Road Test.

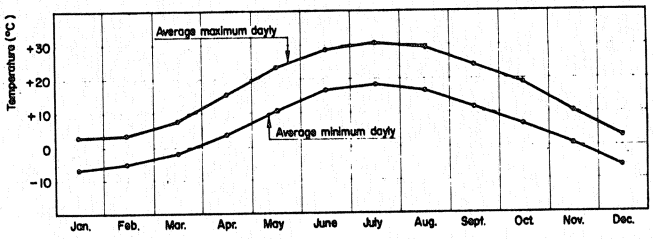

and for the fact that the mean distance from the pavement edge to the outer edge of the dual tire was equal to 62 cm. (2.02 ft).

The following values for input parameters were used:

1. Elastic modulus of concrete: E=32.000 N/mm^2 (4.55x10^6 psi);
2. Poisson coefficient of concrete: μ=0.15;
3. Subbase modulus of reaction: k = variable from 24 N/cm^3 (86 pcd) to 33 N/cm^3 (118 pci) depending on the subbase thickness.

The calculated stresses appear in Table 2.

Not always a comparison between the measured and calculated values has been possible, because in many sections no measured values have been pubblished (18). When possible the calculated stresses of Table 2 resulted in good agreement with the measured one's. The only exception was for section 643 (loop 4, lane 1, h=12.7 cm, 5") where the measured σ_t values were 20 percent lower than the calculated ones. Therefore in our analysis the calculated values were used except for section 643, where the actual measured values were employed.

Temperature Conditions During AASHO Road Test

The maximum and minimum environment air temperatures recorded during the AASHO Road Test are shown in Figure 7.

In the analysis performed, the year was divided in 4 periods each marked by a mean value of the

Table 3. Minimum and maximum values of the air temperature during the AASHO Road Test

Period	Min Air Temp. $\vartheta_{a,min}$ (°C)	Max Air Temp. $\vartheta_{a,max}$ (°C)
Dec.-Jan.-Feb.	- 7	3,5
March 1 - Apr. 15 Oct. 15 - Nov. 30	0	10
Apr. 15 - May 31 Sept. 1 - Oct.15	10	23
June - July - Aug.	17	29,5

Fig. 8 Traffic distribution during the AASHO Road Test.

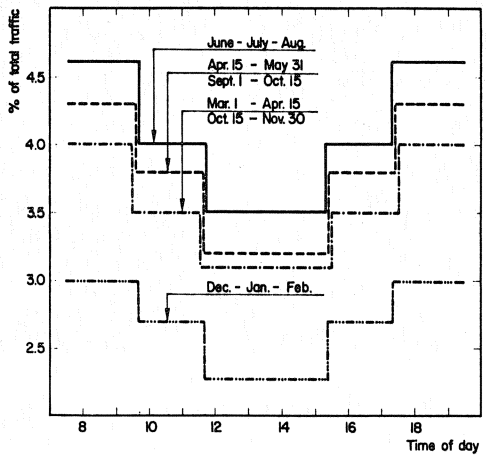

Figure 9. Thermal gradients in AASHO pavements during daytime.

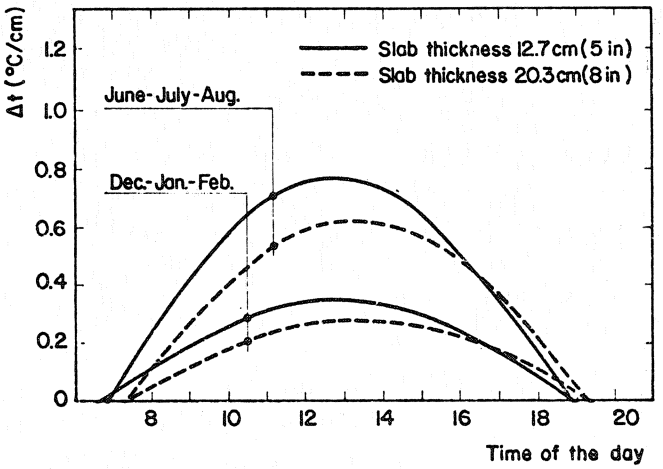

minimum and maximum air temperature. The values used in the calculations are shown in Table 3.

The daily temperature cycle was divided as follows:

1. 1st period: from 07.30 to 09.40
   from 17.20 to 19.30
2. 2nd period: from 09.40 to 11.40
   from 15.20 to 17.20
3. 3rd period: from 11.40 to 15.20

The hours between 19.30 and 07.30 were not considered as in this period the thermal gradients of the slab have negative values. This situation corresponds to 58 per cent of the AASHO daily traffic (14). Figure 8 shows the daytime and yearly traffic distribution values used in the calculations.

Thermal Gradients and Warping Stresses

The stresses induced by the daily temperature variations in the AASHO sections examined have been evaluated by means of Eisenmann's approach (13). As previously said, only warping stresses due to positive thermal gradients have been taken into account. The warping stresses have been calculated for each forementioned year and day period, according to Figure 8.

The calculations of the thermal gradients in the pavements during such periods have been performed assuming that the temperature of the slab surface varies during the day following a sinusoidal law having an amplitude ϑ_o different for each period of the year. The value of the amplitude ϑ_o has been assumed to be a function of the maximum ($\vartheta_{a,max}$) and minimum ($\vartheta_{a,min}$) value of the air temperature, according to the following equation (19):

$$\vartheta_o = \frac{1.5\vartheta_{a,max} - \vartheta_{a,min}}{2} \qquad (7)$$

The values of $\vartheta_{a,max}$ and $\vartheta_{a,min}$ are shown in Table 3. The thermal gradients have been calculated by means of Thomlinson's heat diffusion model (16) by means of the equation:

$$\frac{\Delta T_i}{h} = \frac{\vartheta_o}{h}\left[\sin\frac{2\pi}{T_o}t_i - e^{-\frac{h}{\varphi}\sqrt{\frac{\pi}{T_o}}}\sin\left(\frac{2\pi}{T_o}t_i - \frac{h}{\varphi}\sqrt{\frac{\pi}{T_o}}\right)\right] \qquad (8)$$

in which:

$\Delta T_i/h$ = thermal gradient at the time t_i of the day.

ΔT_i = temperature difference between the surface and the bottom of the slab at the time t_i of the day.

h = thickness of the slab.

T_o = period of temperature cyclic variation (86,400 sec. daily cycle)

t_i = time elapsed from the beginning of daily cycle

φ^2 = diffusivity coefficient of concrete (0.01 sq.cm/sec.)

A typical calculated variation of the thermal gradients during the day time in pavements having slab thickness of 12.7 cm. (5") and 20.3 cm. (8") is shown in Figure 9. The positive values of $\Delta T_i/h$ vary between 0 in the morning at about 7.00 and at about 19.30, and a maximum value at noon. Warping stresses vary accordingly.

Table 4. Thermal gradients ($\frac{\Delta T}{h}$) and warping stresses (σ_w) in AASHO pavements.

Period of the Year		Period of the Day																	
		from 7h30' to 9h40' from 17h20' to 19h30'						from 9h40' to 11h40' from 15h20' to 17h20'						from 11h40' to 15h20'					
		Slab Thickness, cm (in)						Slab Thickness, cm (in)						Slab Thickness, cm (in)					
		6,3 (2,5)	8,9 (3,5)	12,7 (5,0)	16,5 (6,5)	20,3 (8,0)	24,1 (9,5)	6,3 (2,5)	8,9 (3,5)	12,7 (5,0)	16,5 (6,5)	20,3 (8,0)	24,1 (9,5)	6,3 (2,5)	8,9 (3,5)	12,7 (5,0)	16,5 (6,5)	20,3 (8,0)	24,1 (9,5)
Dec.-Jan-Feb.	$\frac{\Delta T}{h}$ (°C/cm)	0,33	0,30	0,24	0,20	0,16	0,13	0,43	0,40	0,35	0,30	0,26	0,23	0,40	0,38	0,35	0,31	0,28	0,25
	σ_w (MPa)	0,26	0,33	0,38	0,41	0,40	0,39	0,34	0,44	0,55	0,61	0,65	0,68	0,31	0,42	0,55	0,63	0,70	0,74
March 1 - Apr. 15	$\frac{\Delta T}{h}$ (°C/cm)	0,42	0,36	0,30	0,24	0,20	0,16	0,53	0,48	0,43	0,37	0,32	0,28	0,50	0,47	0,43	0,39	0,35	0,31
Oct.15-Nov.30	σ_w (MPa)	0,33	0,40	0,47	0,49	0,50	0,48	0,42	0,53	0,67	0,75	0,80	0,83	0,39	0,52	0,67	0,79	0,88	0,92
Apr.15-May 31	$\frac{\Delta T}{h}$ (°C/cm)	0,68	0,60	0,49	0,40	0,32	0,26	0,86	0,79	0,70	0,61	0,53	0,46	0,81	0.77	0,70	0,63	0,57	0,51
Sept.1-Oct.15	σ_w (MPa)	0,53	0,66	0,77	0,81	0,80	0,77	0,67	0,87	1,10	1,24	1,60	1,64	0,63	0,85	1,10	1,28	1,71	1,82
June - July - Aug.	$\frac{\Delta T}{h}$ (°C/cm)	0,75	0,66	0,54	0,44	0,35	0,29	0,95	0,88	0,77	0,67	0,59	0,51	0,90	0,85	0,78	0,70	0,63	0,56
	σ_w (MPa)	0,59	0,73	0,85	0,90	0,88	0,86	0,74	0,96	1,21	1,37	1,77	1,82	0,71	0,93	1,22	1,43	1,90	1,31

The calculated thermal gradients and warping stresses during the chosen periods of the year and day are shown in Table 4.

According to Eisenmann's approach, it may be pointed out that the AASHO rigid pavements, whose slab dimensions were 4.6 x 3.7 (15'x12'), were always in the condition of

$$L > 1.1\, l_{crit}$$

in which:

L = slab lenght or width, according to the position of the critical stress;

l crit.= slab critical lenght in Eisenmann's theory.

The only exception were slabs 20.3 cm and 24.1 cm. thick, in summertime at noon, in which case:

$$0.9\, l_{crit} \leq L \leq 1.1\, l_{crit}$$

or

$$L < 0.9\, l_{crit}$$

The latter limited to one case: h = 24,1 during June-July-August from 11,40 to 15,20 (see Table 4).

Therefore the warping stresses, according to Eisenmann, are given by the equations:

$$\sigma_w = \frac{E\alpha\Delta T}{2(1-\mu)} \quad \text{when} \quad L > 1.1\, l_{crit} \qquad (9)$$

$$\sigma_w = 1.2\frac{E\alpha\Delta T}{2(1-\mu)} \quad \text{when} \quad 0.9\, l_{crit} \leq L \leq 1.1\, l_{crit} \qquad (9')$$

and

$$\sigma_w = \left(\frac{L-40}{0.9\, l_{crit}}\right)^2 \frac{E\alpha\Delta T}{2(1-\mu)} \quad \text{when} \quad L < 0.9\, l_{crit} \qquad (9'')$$

Determination of β Coefficients

The cumulative fatigue damage causing failure produced by the different stress conditions previously calculated for each pavement, and shown in Tables 2 and 4, may be expressed in terms of Miner's law (17). This law, adopting the fatigue relation 6 where β is the unknown, results in the following equation:

$$\sum_i \frac{n_i}{10^{\beta\left(1-\frac{1-\sigma_{i,max}/MR}{1-R_i}\right)}} = 1 \qquad (10)$$

where, besides terms already known:

n_i = number of allowable repetitions for each stress condition, calculated for each type of pavement, from Table 1 and Figure 3.

MR = concrete modulus of rupture equal to 5.8 N / cm^2 (830 psi) for slab thickness 8.9 cm. (3.5") and 5.4 N / cm^2 (770 psi) for all other pavements.

The summation is extended to all stress conditions to which each type of pavement has been subjected, when σ_{max}/MR 0.50. Thus it is

Table 5. Calculated values of β coefficient.

Loop	Lane	Sect.	Thickness cm (in)	N	Σ ni/Ni =0,5 "A"[a]	Σ ni/Ni =0,5 "B"[b]	Σ ni/Ni =1,0 "A"[a]	Σ ni/Ni =1,0 "B"[b]	β aver.
2	2	806	6,3+0 (2,5+0)	300.712	0,0821	0,0682	0,0868	0,0721	0,0773
2	2	814	8,9+0 (2,5+0)	1.017.047	nfd[c]	nfd[c]	nfd[c]	nfd[c]	nfd[c]
4	1	643	12.7+7,6 (5,0+3,0)	644.169	0,1008	0,1060	0,1065	0,1120	0,1063
3	2	220	12,7+22,9 (5,0+9,0)	682.771	0,1195	0,1028	0,1265	0,1085	0,1143
5	1	513	16,5+7,6 (6,5+3,0)	724.686	0,1000	0,0893	0,1058	0,0943	0,0973
6	2	354	20,3+7,6 (8,0+3,0)	1.038.312	0,1390	0,1269	0,1473	0,1342	0,1368
5	1	507	20,3+22,9 (8,0+9,0)	1.110.577	0,1515	0,1416	0,1600	0,1500	0,1508
5	2	508	20,3+22,9 (8,0+9,0)	850.891	0,1700	0,1521	0,1800	0,1611	0,1658
5	1	525	24,1+15,2 (9,5+6,0)	1.220.225	0,2020	nfd[c]	0,2135	ndf[c]	0,2077

[a] "A" : β calculated accounting for $\sigma_{t,\ Westergaard}$ x 0,75 and $\sigma_{w,\ Eisenmann}$

[b] "B" : β calculated accounting for $\sigma_{t,\ Westergaard}$ x 0,75 x 1,15 and σ_w x 0,70

[c] nfd : no fatigue damage

possible to obtain the β coefficient from equation 10 by means of a repetitive process on the basis of the stress values shown in Tables 2 and 4.

In order to examine the influence on β of probable variations in traffic load stresses and warping stresses and of the approximation of Miner's law, β has been calculated also assuming an increase in traffic load stress of 15% (to account for dynamic effects), a decrease in warping stress of 30% (to account for the non linearity of thermal gradients (9) and for the accuracy of Thomlinson's model) and a cumulative damage value causing failure of 0.5.

The results are given in Table 5.

As can be seen, the average variation of β is very limited and does not exceed 10% in the case of stresses and 6% in the case of Miner's law. Therefore a lack of accuracy in the assumptions made can be considered unimportant, and a mean value assumed for β for each pavement type (Table 5).

Analysis of Results

On the other hand the variations of β when the pavement thickness varies is quite consistent.

Comparing the calculated β values with the one proposed by Tepfers (0.0685), it can be seen that the mean calculated value (0.1270) of β is equal to 1.85 times the former, while the maximum calculated value (0.2077) is equal to 3 times the former. This means that, if we assume the average value of β =0.1270, the pavement life would not be consistent with the effective laboratory fatigue behaviour of the concrete, nor with the most severe design fatigue curves proposed up to now. In fact, in this case, for a low stress ratio: $\sigma_{max}/MR = 0.51$ and R variable between 0 and 0.20, the number of allowable load repetitions falls in the range 7,000 - 66,000 compared to the cautions PCA proposed value of 400,000.

This requires an accurate critical examination of the results obtained.

By comparing the calculated β values in Table 5 with the traffic stresses shown in Table 2, it can be noted that β values above 0.11 are associated with low traffic induced stresses, i.e. lower than 0.40 MR. The Authors have deduced that the cracking of these lightely stressed pavements may be due to increased stresses resulting from uncontrollable causes, such as pumping, decrease in dowel or subgrade support efficiency etc., and which can not be accounted for using the fatigue damage model based on calculated initial stress values.

Such uncontrollable phenomena, which require an adequate time in order to show up, probably have not influenced the AASHO pavement behaviour when the thickness is low and traffic induced stresses higher than 0.40 MR, corresponding to β values less than 0.11. The Authors therefore propose that the β values to be used in the fatigue law for the design of concrete pavements should be obtained using only values lower than 0.11.

Proposed Fatigue Law

The average value of β coefficients lower than 0.11 equals 0.0954.

Referring to relation 6, the proposed fatigue law can be thus presented in the following way:

$$\frac{\sigma_{max}}{MR} = 1 - 0.0954(1-R)\log_{10} N \qquad (11)$$

Figure 10. Fatigue curves proposed for plain concrete pavement design

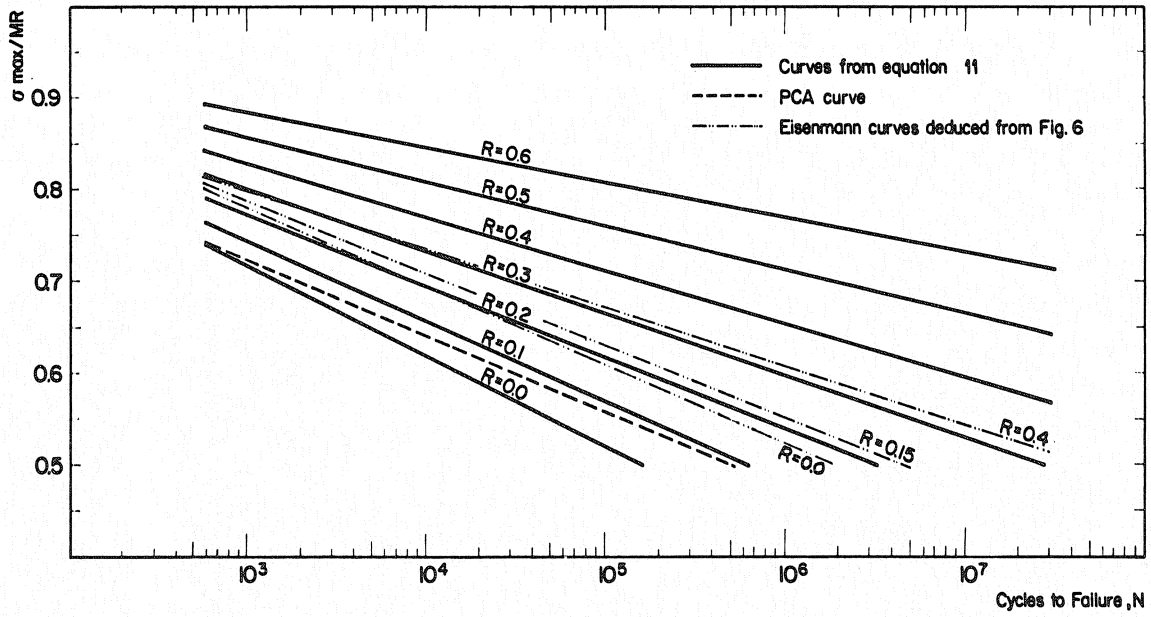

Figure 11. Goodman-Smith diagram obtained on the basis of the fatigue law 11.

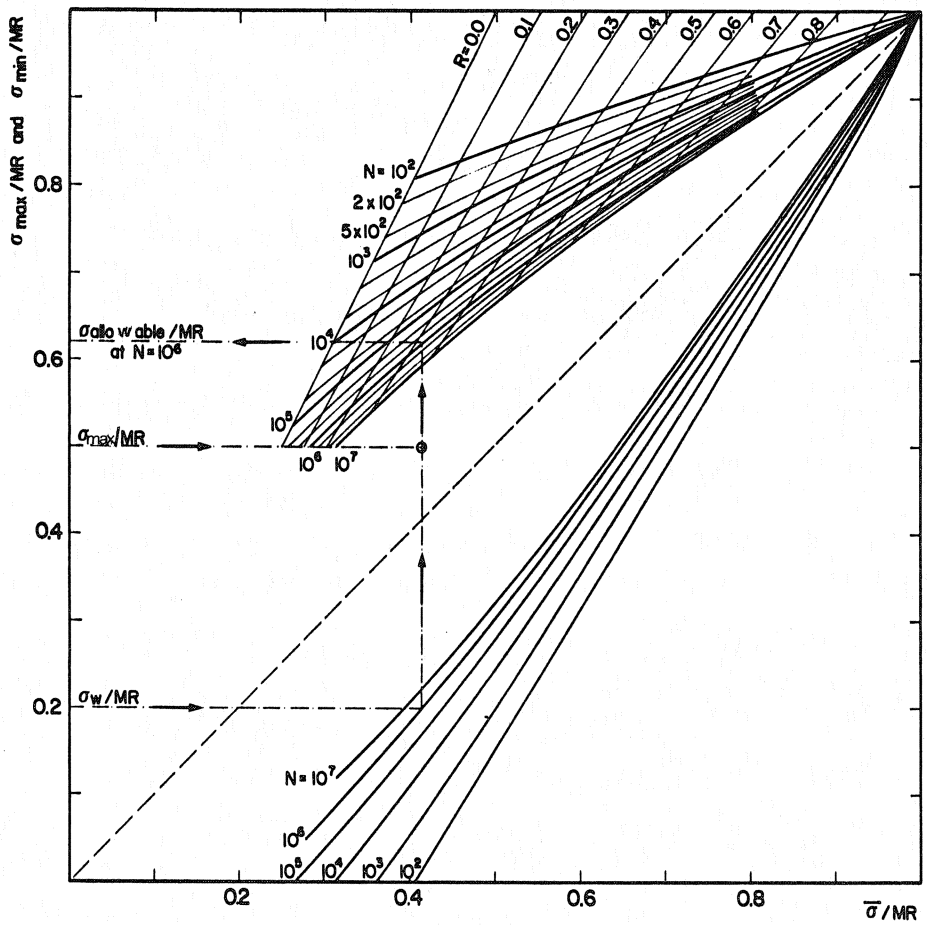

The respective fatigue curves, where R = const., are shown in the Wholer diagram of Figure 10. For comparison purpose, the PCA proposed curve (3) and the curves at R = costant deduced from the modified Goodman-Smith diagram proposed by Eisenmann (13) have also been included in Figure 10.

Applying the equation 11 to the AASHO pavements which in the previous analysis gave β values higher than 0.11 and which have not been averaged, it can be deduced that, to justify the fatigue failure of such pavements, the effects of the forementioned uncontrollable phenomena can be assumed to correspond to an encrease of the initial calculated traffic stresses of about 40-50%.

The modern trend of stabilizing the subbase and providing adeguate drainage to minimize such uncontrollable phenomena, in the Authors opinion extends the applicability of the fatigue model based on calculated stresses and equation 11 also to the design of pavements thicker than those assumed in the determination of the β coefficient.

The fact that PCA and Eisenmann curves fall within the proposed fatigue damage curves calculated with β =0.0954 supports this assumption. As a matter of fact, the PCA curve, defined on the basis of the most severe experimental results obtained by laboratory tests with R < 0.15, falls within the calculated curves with R=0 and 0.1; on the other hand, the Eisenmann curves are less conservative for R < 0.2 and more conservative for R > 0.4.

Finally, from Figure 10 it can be noted that the allowable loads repetitions with a stress ratio equal, for instance, to 0.51 increase from approximately 140.000, corresponding to a stress condition with R=0, to 2,500,000 with R=0.2. This suports the importance to adopt Rmin values higher than zero and, consequently, as previously demonstrated, safety factors respect to traffic loads higher than 2.

The graphical representation, using the Goodman-Smith diagram, of the proposed fatigue law is shown in Figure 11. The diagram shows only the allowable stress conditions $\sigma_{min} \geq 0$ (i.e. $R \geq 0$) and $\sigma_{max}/MR > 0.5$. The Goodman-Smith diagram allows for a more immediate identification of the allowable σ_{max} as a function of σ_{min} when N is known. Therefore it may be useful at a preliminary design phase, for the choise of the pavement slab dimensions. Having chosen a particular slab thickness and lenght, thus setting a σ_{min} value, it will be possible to define a fatigue safety coefficient respect to traffic load stress increases, as a function of the foreseen repetitions at maximum load. For example, in Figure 11, assuming $\sigma_w/MR=0.20$; $N = 10^6$ and $\sigma_t/MR=0.30$ we obtain $\sigma_{max}/MR=0.50$ with a safety coefficient equal to 1.24. These calculations may be useful, for example, when the transit of over loaded trucks may be foreseen.

Conclusions

1. In order to correctly interpret the fatigue behaviour of plain concrete pavements, the Authors propose in the design procedure to take into consideration the effect of the stress range as this parameter has a marked influence on concrete fatigue resistance. Stress conditions with a high stress range (i.e. low values of $R = \sigma_{min} / \sigma_{max}$) result in more severe effects than stress conditions with high R values. Therefore, in designing, if only traffic loads are considered, a safety coefficient higher than 2 should be adopted in order to obtain values of Rmin. higher than zero (for example, with a safety factor = 2.5, Rmin.= 0.20).

2. The fatigue law which the Authors propose to be used in the fatigue design is given by equation 11.

This relationship, obtained by correcting on the basis of the AASHO Road Test results the laboratory concrete fatigue law 6, is more conservative than the latter. This is necessary because the behaviour of actual pavements is less controllable than the behaviour of concrete in the laboratory.

3. The fatigue law 11 relates to a pavement Cracking Index equal to 0.16 m/ m^2 (50 ft/sq.ft). A pavement designed with such a fatigue law has a useful residual life of approximately 25 to 30 per cent.

4. To account for a possible encrease of the initial traffic stresses due to a loss of subgrade support, an encrease up to 150% of the calculated stress values can be adopted.

References

1. R. TEPFERS. Tensile Fatigue Strength of Plain Concrete. ACI Journal, August 1979.
2. R. TEPFERS and T. KUTTI. Fatigue strength of Plain, Ordinary and Lightweight Concrete. ACI Journal, May 1979.
3. P.C.A. Thickness Design for Concrete Pavements. 1966, Skokie, Ill.
4. G. PICKETT and G.K. RAY. Influence Charts for Concrete Pavements. Trans. ASCE, vol. 116, 1951.
5. R.G. PACKARD. Fatigue Concepts for Concrete Airport Pavements Design. Proc. ASCE, Trasp. Eng. Jour., n. TE3, 1974.
6. M.I. DARTER and E.J. BARENBERG Zero-Maintenance Design for Plain Jointed Concrete Pavements. Proc. Int. Conf. on Concrete Pavement Design, Purdue, Feb. 1977.
7. S. IWAMA Experimental Studies on the Structural Design of Concrete Pavements. Pav. Lab., Public Works Research Inst., Ministry of Construction, Japan, May 1974.
8. P. FERRARI and F. GIANNINI. Ingegneria Stradale, vol. II. Corpo Stradale e Pavimentazioni, Ed. ISEDI, Milano, 1979.
9. L. DOMENICHINI. Influenza delle sollecitazioni da Inflessione Termica sul Dimensionamento delle Pavimentazioni Rigide. Proc. XVIII Convegno Nazionale Stradale, Italia, Taormina, June 1978.
10. ACI Committee 215. Considerations for Design of Concrete Structures Subjected to Fatigue Loading. ACI Jour., March 1974.
11. C.A. BALLINGER. Cumulative Fatigue Damage Characteristics of Plain Concrete. HRB Rec. 370, 1971.
12. C.E. KESLER. Effect of Speed of Testing on Flexural Fatigue Strenght of Plain Concrete. Proc. HRB, vol. 32, 1963.
13. J. EISENMANN. Bemessung Von Zementbetondecken. Forschunsarbeiten aus den Strassenwesen, n° 82, Kirschbaum Verlag, July 1970.
14. The AASHO Road Test. HRB Spec. Rep. 61 (7 reports), 1961-1962.
15. H.M. WESTERGAARD. New Formulas for Stresses in Concrete Pavements for Airfields. Trans. ASCE, vol. 113, 1948.
16. J. THOMLINSON. Temperature Variations and Conseq-uent Stresses Produced by Dayly an Seasonal Temperature Cycles in Concrete Slabs. Concrete and Constructional Engineering (London), vol. 35, June-July 1940.
17. M.A. MINER. Cumulative Damage in Fatigue. Trans. ASME, vol. 67, 1945.
18. A.S. VESIC and S.K. SAXENA. Analysis of Structural Behaviour of AASHO Road Test Rigid Pavements. NCHRP Report 97, 1970.
19. V. VENKATASUBRAMANIAN. Temperature Variations in a Cement Concrete Pavement and the Underlaying Subgrade. HRB Rec. 60, 1963.